(1990); A. Guirao, M. Pi, M. Barranco, *ibid.* **D21**, 185 (1991).
14. M. Hartmann, F. Mielke, J. P. Toennies, A. Vilesov, G. Benedek, *Phys. Rev. Lett.* **76**, 4560 (1996).
15. D. S. Betts, D. W. Osborne, B. Welber, J. Wilks, *Philos. Mag.* **8**, 977 (1963).
16. A. D. B. Woods and A. C. Hollis-Hallet, *Can. J. Phys.* **41**, 596 (1963).
17. M. Hartmann, thesis, University of Göttingen, Göttingen, Germany (1997) (available as Bericht 10/1997 from Max-Planck-Institut für Strömungsforschung, Göttingen, Germany).
18. D. O. Edwards, M. S. Pettersen, T. G. Culman, *J. Low Temp. Phys.* **89**, 831 (1992).
19. M. Barranco, M. Pi, S. M. Gatica, E. S. Hernandez, J. Navarro, *Phys. Rev. B* **56**, 8997 (1997).
20. S. Grebenev, M. Hartmann, M. Havenith, J. P. Toennies, A. F. Vilesov, in preparation.
21. The laser beam, produced by a Mütek MSD 1100 diode laser ($\lambda \cong 5\mu$, resolution $\delta\nu \lesssim 100$ MHz), was directed coaxially but antiparallel to the droplet beam through a BaF_2 window at the far end of the apparatus.
22. J. Harms and J. P. Toennies, in preparation. The method used is described by M. Lewerenz, B. Schilling, and J. P. Toennies [*Chem. Phys. Lett.* **206**, 381 (1993)].
23. J. H. R. Clarke, in *Advances in Infrared and Raman Spectroscopy 4* (Heyden, London, 1978), chap. 4, pp. 109–193.
24. R. G. Gordon, *J. Chem. Phys.* **44**, 1830 (1966).
25. In quantum solids such as H_2, the rotors behave as if they were free, and sharp rotational spectral features have been observed [P. J. Berkhout and I. F. Silvera, *Commun. Phys.* **2**, 109 (1977); M. Okumara, M. C. Chan, T. Oka, *Phys. Rev. Lett.* **62**, 32 (1989)].
26. M. Lewerenz, B. Schilling, J. P. Toennies, *J. Chem. Phys.* **102**, 8191 (1995).
27. The weak interaction at the ^{4}He-^{3}He interface is consistent with the very small surface tension measured at the interface [H. M. Guo, D. O. Edwards, R. E. Sarwinski, J. T. Tough, *Phys. Rev. Lett.* **27**, 1259 (1971)].
28. Y. Kwon, D. M. Ceperley, K. B. Whaley, *J. Chem. Phys.* **104**, 2341 (1996).
29. M. Chester and L. C. Yang, *Phys. Rev. Lett.* **31**, 1388 (1973).
30. H. Lamb, *Hydrodynamics* (Dover, New York, ed. 6, 1945), p. 154.
31. We thank J. Harms, B. Sartakov, and Y. Kagan for valuable discussions on ^{3}He droplets; G. Benedek, J. Close, Y. Kagan, and B. Whaley for reading and commenting on the manuscript; and S. Bartolomei and M. Lewerenz for preparing Fig. 3. A.V. thanks the Deutsche Forschungsgemeinschaft for a "habilitation stipendium."

8 October 1997; accepted 13 January 1998

Elevation Change of the Southern Greenland Ice Sheet

Curt H. Davis,* Craig A. Kluever, Bruce J. Haines

Seasat and Geosat satellite altimeter measurements for the Greenland ice sheet (south of 72°N latitude) show that surface elevations above 2000 meters increased at an average rate of only 1.5 ± 0.5 centimeters per year from 1978 to 1988. In contrast, elevation changes varied regionally from −15 to +18 centimeters per year, seasonally by ±15 centimeters, and interannually by ±8 centimeters. The average growth rate is too small to determine if the Greenland ice sheet is undergoing a long-term change due to a warmer polar climate.

Understanding the current state of the polar ice sheets is critical for determining their contribution to sea-level rise and predicting their response to climate change. Current estimates from decades of tide-gauge data indicate an increase in global sea level of 10 to 20 cm over the past century (*1*). It is uncertain, however, what the individual contributions of the polar ice sheets are to sea-level rise at this time. The Greenland ice sheet is of particular interest in climate change studies because it is significantly warmer than the Antarctic ice sheet, where temperatures remain well below freezing over the majority of its surface. Also, the potential for polar amplification of a global warming trend in the Northern Hemisphere is very likely (*2*). Thus, the Greenland ice sheet is likely to undergo more dramatic change in response to a global warming trend.

Using satellite radar altimeter data from the Seasat and Geosat missions, Zwally *et al.* (*3*) estimated that the southern part of the Greenland ice sheet (south of 72°N latitude) grew by 23 ± 6 cm/year from 1978 to 1986. Zwally (*4*) suggested an increase in precipitation rates caused by a warmer polar climate as a possible cause of the volume growth. However, concerns have been raised about the effect of orbit errors, retracking errors, and systematic biases on these results (*5–8*). We reexamined elevation change of the Greenland ice sheet, using Seasat and Geosat altimeter data through 1988 after incorporating recent technical advancements in ice-sheet retracking, orbit computation, and orbit error reduction.

The Seasat and Geosat altimeters were designed primarily for measuring sea-surface height. Altimeter data collected over the ice sheets must be postprocessed to produce accurate surface elevation measurements. This is called "retracking" and is required because the leading edge of the reflected radar signal deviates from the tracking gate on the satellite, causing an error in the range measurement. Comparison of the repeatability of surface elevations produced from different ice-sheet retracking algorithms (*7*) showed that the retracking algorithm (*9*) used by Zwally *et al.* (*3*), hereafter referred to as the NASA algorithm, introduced larger errors in the elevation data than did three other retracking algorithms. Also, the NASA algorithm produced ice-sheet growth rate estimates 30 to 50% larger than those derived from three competing algorithms, which all produced nearly identical results. Although several refinements of the NASA algorithm have now been made (*10*), it still introduces significant random error in ice-sheet datasets. We used a threshold retracking algorithm developed specifically for measurement and detection of ice-sheet elevation change (*11*). The threshold algorithm reduces random errors in ice-sheet data by up to 35% compared to the current NASA algorithm (*11*).

For comparing Seasat and Geosat data, Zwally *et al.* (*3*) used orbit solutions accurate to about 1 m in the radial component (*12*). The solutions for Seasat and Geosat were derived from different gravity models. Because of this and other factors, these authors used a 40 ± 40 cm systematic correction in their analysis. Since then, several consistent sets of orbit solutions have been developed for both datasets. We used Joint Gravity Model–3 (JGM-3) (*13*) orbit solutions that are now available for Seasat, Geosat-Geodetic Mission (GM), and the Geosat-Exact Repeat Mission (ERM) satellite datasets. The radial component of Geosat JGM-3 orbits is accurate to 10 cm (*14*). The Seasat JGM-3 orbits, while not as accurate as their Geosat counterparts, represent significant improvement over previous solutions.

Most studies of ice-sheet elevation change correct altimeter radial orbit error using a reference ocean surface in the vicinity of the ice sheet (for example, the North Atlantic for Greenland) (*15*). However, the predominant radial orbit error is a long-wavelength signal concentrated at a frequency of 2π/orbital period (1/rev frequency). Within each continuous orbit solution, the phase and amplitude of the 1/rev error change gradually over large distances, where a high level of correlation is main-

C. H. Davis, Department of Electrical Engineering, University of Missouri, 5605 Troost Avenue, Kansas City, MO 64110, USA.
C. A. Kluever, Department of Mechanical and Aerospace Engineering, University of Missouri, 5605 Troost Avenue, Kansas City, MO 64110, USA.
B. J. Haines, Jet Propulsion Laboratory, California Institute of Technology, 4800 Oak Grove Drive, Pasadena, CA 91109, USA.

*To whom correspondence should be addressed. E-mail: curt@polar.cuep.umkc.edu

Table 1. SD of crossover residuals for uncorrected and corrected datasets. The statistics are based on height differences at crossover points. Ocean datasets are from the North Atlantic region (56° to 72°N latitude, 290° to 360°E longitude). The root-difference-square (RDS) is a measure of the magnitude of the orbit-error reduction. RDS is the square root of the difference between the squares of the uncorrected and corrected SD.

Dataset	Uncorrected SD (cm)	Corrected SD (cm)	RDS (cm)
Seasat ocean	27.5	13.0	24.2
Geosat ocean	10.0	8.6	5.0
Geosat × Seasat ice	44.5	36.9	24.9

Table 2. ERM × Seasat elevation change results; *n*, number of satellite track crossover points.

Dataset	Regular *dH*/*dt* analysis				Spatial *dH*/*dt* analysis			
	dH (cm)	*dt* (years)	*n*	*dH*/*dt* (cm/year)	*dH* (cm)	*dt* (years)	*n*	*dH*/*dt* (cm/year)
87 × S	15 ± 7	9	4,277	1.7 ± 0.8	22 ± 7	9	3,539	2.4 ± 0.8
88 × S	22 ± 12	10	2,789	2.2 ± 1.2	2 ± 12	10	1,908	0.2 ± 1.2
ERM × S	8 ± 3	9.25	32,867	0.9 ± 0.3	19 ± 5	9.25	32,283	2.0 ± 0.5

tained from one orbit revolution to the next (*16*). A global analysis of ocean altimeter data is better suited to exploit these characteristics and can be used to separate 1/rev orbit errors from global measurement system biases that may be present when comparing data from different satellites (for example, Geosat × Seasat). Equally important, orbit corrections derived from a global analysis are less likely to absorb signals from actual regional sea-level variations and inaccurately modeled sea-state and atmospheric pressure loading effects at high latitudes.

We used the Seasat (6 July to 10 October 1978) and Geosat-ERM (8 November 1986 to 7 November 1988) global ocean altimeter datasets from the NASA Ocean Altimeter Pathfinder program (*17*) for our orbit error analysis. We created ocean residuals by differencing Seasat and Geosat sea-surface heights with a global reference network of mean ERM profiles (*18*). The residuals were processed by a stochastic filter to estimate radial orbit error and global bias coefficients (*19*). Only a modest reduction in radial orbit error was obtained for the Geosat-ERM ocean data because of the high quality of the orbit solutions (*13, 14*). In contrast, a substantial reduction in radial orbit error was obtained for the Seasat ocean data (Table 1). The reasons behind the larger magnitude of the Seasat radial orbit error are not fully understood, but the poorer quality and limited geographic distribution of the satellite tracking data likely contribute. Evaluation of the global bias coefficients showed that Seasat sea levels were, on average, 27 cm lower than those from Geosat-ERM (*20*). Because global mean sea-level rise during the period between Seasat and Geosat could account for only about 2 cm, we attribute the 27-cm difference primarily to measurement system bias between the two satellites (*21*).

We used the Seasat and Geosat-ERM Greenland datasets from the NASA Ice Sheet Altimeter Pathfinder program (*22*). Both satellites provided coverage up to a maximum latitude of 72°N. The ice-sheet surface elevations were produced using the same JGM-3 orbit solutions applied to the ocean altimeter datasets. Orbit error and global bias corrections from evaluation of the ocean data were applied to the ice-sheet elevations. Nearly identical reductions in radial orbit error were obtained for the ice-sheet data and ocean data from the North Atlantic (Table 1) (*23*). Because ice-sheet data were not used in the orbit error analysis, this demonstrates that the stochastic filter was very effective in removing radial orbit error without absorbing significant sea-level signal. Ice-sheet elevation differences were computed at crossover points between the ERM and Seasat satellite tracks. A small correction was applied to each elevation difference to correct for slight altitude differences between the two satellites (*24*).

For two datasets (87 × S, 88 × S), we used the same 3-month time period in both the Seasat (1978) and ERM (1987 and 1988) data to avoid seasonal biases. For a third dataset (ERM × S), we used the first 2 years of ERM data with the Seasat data to provide a larger number of crossovers (*n*), a better spatial distribution, and to average

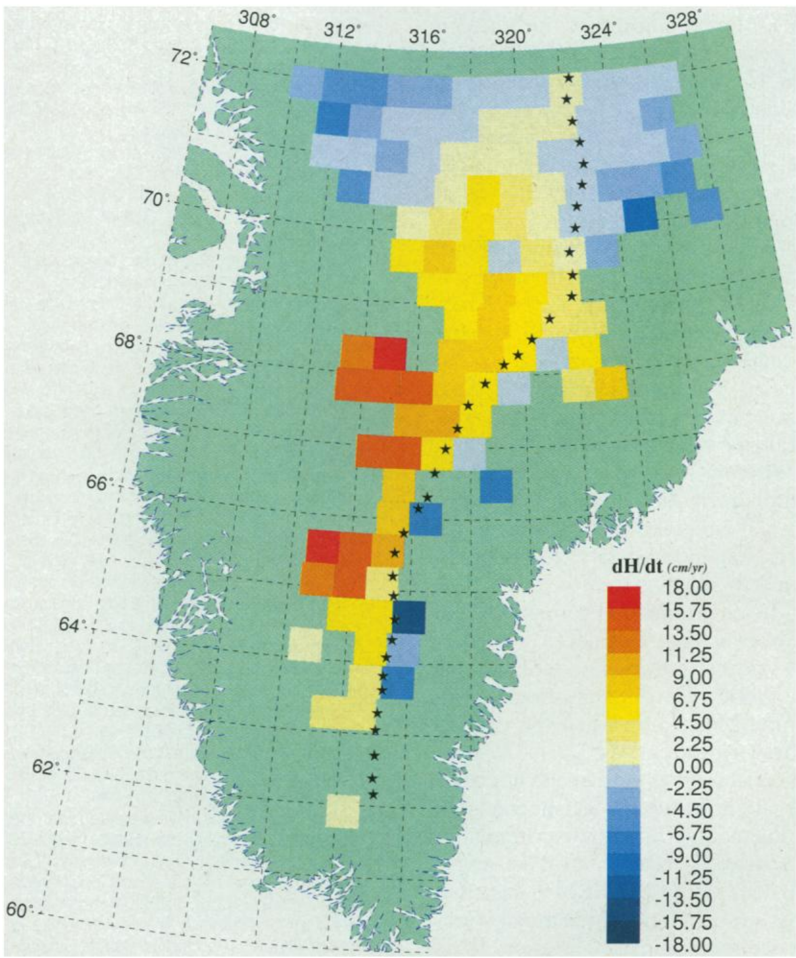

Fig. 1. Spatial distribution of elevation change from 1978 to 1988 showing large variations in *dH*/*dt* values. The approximate location of the ice divide is indicated by the series of stars. A spatial average yields a growth rate of 2.0 ± 0.5 cm/year.

out seasonal variations. We considered both the average change in elevation (dH) divided by the average time interval (dt), using all the crossovers (*25*) and a spatial average of the data in 50 km by 50 km cells (*26*). A spatial analysis is required because most of the satellite tracks are located in the northern interior of the ice sheet (*4*). The results for all datasets are consistent and give growth rates of 1 to 3 cm/year (Table 2). These rates are significantly smaller than the rate inferred by Zwally *et al.* (*3*).

Analysis of the spatial distribution of the crossover data indicates that the rate of change varies from –15 to +18 cm/year across the ice sheet (Fig. 1). Changes in the northern interior of the ice sheet are small (–2 to +2 cm/year) and are consistent with estimates showing no significant change in mass balance (*27*). Thinning of 3 to 10 cm/year is indicated for the lower elevations of the eastern and western flanks of the ice sheet between 70° to 72°N. The ice sheet west of the ice divide between 65° to 69°N increased in elevation by 10 to 15 cm/year. This rate agrees with growth rates derived from a comparison of airborne laser altimeter and ground survey data from 1980 to 1994 (*28*). Modest thinning is indicated in a few places east of the ice divide between 63° to 67°N, which is also consistent with laser altimeter results (*28*). However, confidence is low here because of poor spatial coverage. In contrast, Zwally (*4*) reported large growth rates (>20 cm/year) for all elevation and latitude bands.

The spatially averaged result for the southern Greenland ice sheet from 1978 to 1987–88 is 2.0 ± 0.5 cm/year. After correcting for vertical crustal motion (*29*), the spatially averaged growth rate is 1.5 ± 0.5 cm/year. The 0.5 cm/year uncertainty accounts for only the random component of the error. Application of orbit error corrections from extreme filtering strategies suggests that the systematic contribution from residual orbit error is <0.5 cm/year. Uncertainties in the vertical crustal motion, knowledge of the relative measurement system bias (*30*), and biases in the environmental corrections likely contribute at the same level. Thus, the small 1.5 cm/year growth rate estimate may not be significantly different from a null growth rate. Most (>95%) of the data we used is from elevations >2000 m. We can make no conclusion as to the behavior of the lower elevations nearer the ice-sheet margin. Natural fluctuations in snow accumulation rates can cause decadal changes in surface elevation (*8*). Using the ERM dataset, we estimated seasonal and interannual variations in ice-sheet surface elevation to be ±15 cm and ±8 cm, respectively (*31*). Considering the large spatial and temporal variations, the 1.5 ± 0.5 cm/year growth rate is too small to assess whether or not the Greenland ice sheet is undergoing a long-term change due to a warmer polar climate.

REFERENCES AND NOTES

1. B. C. Douglas, *Rev. Geophys. (Suppl.)* **33**, 1425 (1995).
2. E. Barron, *USGCRP Report 95-02* (U.S. Global Change Research Program, Washington, DC, 1995).
3. H. J. Zwally, A. C. Brenner, J. A. Major, R. A. Bindschadler, J. G. Marsh, *Science* **246**, 1587 (1989).
4. H. J. Zwally, *ibid.*, p. 1589.
5. B. C. Douglas, R. E. Cheney, L. Miller, R. W. Agreen, *ibid.* **248**, 288 (1990).
6. H. J. Zwally, A. C. Brenner, J. A. Major, R. A. Bindschadler, J. G. Marsh, *ibid.*, p. 288.
7. C. H. Davis, *IEEE Trans. Geosci. Remote Sens.* **33**, 1108 (1995).
8. C. J. Van der Veen, *Clim. Change* **23**, 383 (1993).
9. T. V. Martin, H. J. Zwally, A. C. Brenner, R. A. Bindschadler, *J. Geophys. Res.* **88**, 1608 (1983).
10. For example, H. J. Zwally, A. C. Brenner, J. DiMarzio, T. Seiss, *Proceedings of Second ERS-1 Symposium ESA SP-361*, Hamburg, Germany, 11 to 14 October 1993 (European Space Agency, 1994), p. 159; see also (*22*).
11. C. H. Davis, *IEEE Trans. Geosci. Remote Sens.* **35**, 974 (1997).
12. J. G. Marsh and R. G. Williamson, *J. Astronaut. Sci.* **87**, 3207 (1982); S. Smith III, G. West, C. Malyevac, *Johns Hopkins APL Tech. Dig.* **8**, 198 (1987).
13. B. D. Tapley *et al.*, *J. Geophys. Res.* **101**, 28209 (1996).
14. The Geosat JGM-3 orbit solutions show subdecimeter accuracy in colinear ocean altimeter data [F. G. Lemoine *et al.*, *Eos (Spring Suppl.)* **78**, 103 (1997)] and comparisons of monthly averaged tide gauge and altimeter sea level differ at the level of a few centimeters (http://ibis.grdl.noaa.gov/SAT/gdrs/geosat_handbook/docs/chap_1.htm).
15. For example, H. J. Zwally *et al.*, *NASA Ref. Publ. 1233* (NASA, Washington, DC, 1990), vol. 1; C. S. Lingle *et al.*, *Ann. Glaciol.* **20**, 26 (1994).
16. D. B. Chelton and M. G. Schlax, *J. Geophys. Res.* **98**, 12579 (1993).
17. Ocean Altimeter Pathfinder home page, http://neptune.gsfc.nasa.gov/ocean.html
18. Residuals were formed at the intersection (crossover points) between the satellite ground tracks and the reference network. The reference network was created by averaging the first 2 years of colinear ERM sea heights after correcting for orbit errors. Only the first 2 years of ERM data were used, because the accuracy of the orbit solutions were severely degraded by solar activity beginning in the third year.
19. The radial orbit errors, $E(t)$, within each orbit solution (typically 6 days) were parameterized by $E(t) = A(t)\cos\Omega t + B(t)\sin\Omega t + C$, where $\Omega = 2\pi$/orbital period. In the stochastic filter [S. M. Lichten, *Manuscripta Geodaetica* **15**, 159 (1990)], the 1/rev orbit-error amplitudes, $A(t)$ and $B(t)$, were treated as exponentially correlated noise processes with a time constant of 6 days [C. A. Kluever, B. J. Haines, C. H. Davis, Y. T. Yoon, *Eos (Spring Suppl.)* **78**, 103 (1997)]. The bias parameter, C, was held constant over each 6-day Seasat orbit solution and was used to account for a global-scale difference between Seasat and Geosat sea heights because of measurement-system biases.
20. There were 17 separate 6-day Seasat orbit solutions used in our study. The mean and SD of the Seasat bias coefficients were 27 ± 4 cm.
21. Other investigations have indicated that the Seasat altimeter yielded lower sea-surface heights relative to Geosat [B. Haines, thesis, University of Colorado, Boulder (1991); C. Wagner and R. Cheney, *J. Geophys. Res.* **97**, 15607 (1992)]. A recent independent study by G. Kruizinga [thesis, University of Texas, Austin (1997)] reported a Seasat-Geosat relative bias of 22 ± 4 cm.
22. Ice-Sheet Altimeter Pathfinder home page, http://crevasse.stx.com/ia_home/
23. The root-difference square (RDS) for the Geosat × Seasat ice-sheet data is 24.9 cm, which is nearly identical to the combined RDS for the Seasat and Geosat ocean data, that is $\sqrt{24.2^2 + 5.0^2} = 24.7$ cm.
24. The nominal orbit altitude for both Seasat and Geosat was 800 km, but small differences between the orbital heights (±5 km) did occur at a given point on the ice-sheet surface. Over a flat surface, the change in elevation computed from two different satellites (A and B) is $dH = H_B - H_A$, where H_B and H_A are the surface elevations located at the same point (nadir) on the ice-sheet surface. Over a sloping ice-sheet surface, the location of the closest point to the surface will be different for satellites with different orbital heights. In this case, $dH = H_B - \Delta - H_A$, where the correction $\Delta = (OH_B - OH_A)(1 - \cos\alpha)$, OH are the orbital heights, and α is the regional ice-sheet slope. The regional slope was determined using a 10 km by 10 km grid computed from a digital elevation model of Greenland produced by S. Ekholm at Kort-og Matrikelstyrelsen, Denmark. The mean and SD of all corrections applied to 35,600 ERM × Seasat dH values was –1.4 ± 4.6 cm.
25. The ascending-descending (A-D) orbit bias is accounted for by using the method described by Zwally *et al.* (*3*). Crossover differences greater than 3 SD of the primary Gaussian distribution were discarded to eliminate data outliers due to irregular ice-sheet topography; see note 8 in (*3*).
26. An average dH and dt value was computed for each cell before computing the spatial average of all cells. For a cell to be used, a minimum of 10 crossovers had to be present, with at least five from Geosat-Seasat (A-D) and five from Seasat-Geosat (A-D).
27. J. F. Bolzan, *Eos (Fall Suppl.)* **73**, 203 (1992).
28. W. Krabill, R. Thomas, K. Jezek, K. Kuivinen, S. Manizade, *Geophys. Res. Lett.* **22**, 2341 (1995).
29. A correction for vertical velocity of the ice base because of crustal deformation was subtracted from the dH/dt value of each 50 km by 50 km cell, and the spatial average was recalculated (see http://cfageod4.harvard.edu/calc_def.html for details of the vertical velocity calculations).
30. The relative measurement system bias (*20, 21*) is estimated from the global ocean data and as such is not perfectly separable from the sea-state bias (SSB) resulting from the noncoincidence of electromagnetic and geometric sea level as well as tracker and skewness biases. Although the SSB model for the Geosat data has been rigorously estimated [P. Gaspar, F. Ogor, and M. Hamdaoui, http://neptune.gsfc.nasa.gov/~krachlin/opf/algorithms/ssb_geosat.html], the corresponding model for the Seasat data is still under investigation. Older models [for example, G. H. Born, M. A. Richards, G. W. Rosborough, *J. Geophys. Res.* **87**, 3221 (1982)] may not be appropriate because the Seasat data have been retracked as part of the Pathfinder effort (*17*). We estimated a global SSB for Seasat as a percentage of the significant wave height (SWH). Conservatively assuming our estimate of 0.044 × SWH is accurate to within 40%, the relative measurement system bias would be accurate to ~5 cm (global SWH averages 2.7 m). A 5-cm error in the relative bias translates to 0.5 cm/year in terms of the overall ice-sheet growth rate.
31. The seasonal signal cycle is approximately sinusoidal and is observed in monthly variations in the dH values over the 2-year period. Interannual variations were computed by subdividing each year of data into four 3-month seasonal periods and performing a same-season crossover analysis (for example, Fall 1988 × Fall 1987).

32. We thank R. Thomas for suggesting the satellite height correction (*24*). We thank the NASA Pathfinder Program for the ocean and ice sheet altimeter datasets; in particular, we acknowledge the help of H. J. Zwally, C. Koblinsky, A. Brenner, J. DiMarzio, and B. Beckley for their assistance in obtaining these data. We thank C. Perez and Y. Yoon for processing the data for this study. Supported by NASA's Polar Program and the Office of Mission to Planet Earth under grants NAGW-5010 and NAGW-5243. A portion of this work was conducted by the Jet Propulsion Laboratory, California Institute of Technology, under contract with NASA on RTOP #622-83-1740.

2 September 1997; accepted 9 February 1998